Numerical studies of nonlocal electrostatic effects on the sub-nanoscale

2009 J. Phys.: Condens. Matter 21 255901

(http://iopscience.iop.org/0953-8984/21/25/255901)

IOP PUBLISHING JOURNAL OF PHYSICS: CONDENSED MATTER

J. Phys.: Condens. Matter **21** (2009) 255901 (7pp) doi:10.1088/0953-8984/21/25/255901

Numerical studies of nonlocal electrostatic effects on the sub-nanoscale

Jörg Rottler and B Krayenhoff

Department of Physics and Astronomy, University of British Columbia, 6224 Agricultural Road, Vancouver, BC, V6T 1Z1, Canada

E-mail: jrottler@phas.ubc.ca

Received 29 November 2008, in final form 5 May 2009
Published 27 May 2009
Online at stacks.iop.org/JPhysCM/21/255901

Abstract

We study nonlocal electrostatics in inhomogeneous dielectric environments on the sub-nanometer scale using a recently introduced polarization energy functional. This functional is able to generate a wavevector-dependent dielectric function $\epsilon(\mathbf{q})$ that reflects local correlations in the medium's polarization. Its longitudinal component either decays continuously from its macroscopic continuum value to one at large q, or additionally exhibits two poles with a negative band at intermediate wavevectors (overscreening), which is characteristic of polar fluids such as water. We show that the functional reproduces known nonlocal electrostatic effects: the pair potential between point charges or Born ions in water at distances less than 5 Å is strongly modified, and the Born solvation energy is found to either decrease or increase relative to its local electrostatics value, depending on which approximation is chosen for $\epsilon(\mathbf{q})$. We then apply the functional to geometries that can no longer be treated analytically, such as a molecular pore of finite length. In such an anisotropic dielectric background transverse correlations in the polarization field no longer vanish and can contribute to substantial modifications of the dielectric barrier for ion translocation in the regime of intermediate pore diameters of 6–10 Å.

1. Introduction

The conventional theory of dielectric response in continuous media is based on a local, linear relationship between the dielectric displacement field $\mathbf{D}$ and the electric field $\mathbf{E}$ mediated by the dielectric permittivity $\epsilon(\mathbf{r})$, $\mathbf{D}(\mathbf{r}) = \epsilon(\mathbf{r})\mathbf{E}(\mathbf{r})$ [1]. Underlying this approach is the assumption that correlations in the polarization field $\mathbf{P} = \mathbf{D} - \mathbf{E}$ are absent and a purely local susceptibility $\chi(\mathbf{r})$ suffices to describe the response to an electric displacement, $\mathbf{P}(\mathbf{r}) = \chi(\mathbf{r})\mathbf{D}(\mathbf{r})$. While this is usually a good approximation for macroscopic objects, it does not accurately describe liquids on the sub-nanometer scale. In a highly polar fluid such as water, for instance, the orientation of the dipole moment of a water molecule is strongly dependent on the orientation of the molecules in the immediate neighborhood. In order to describe such correlations, one must assume that the dielectric response is nonlocal and the dielectric function depends on two spatial arguments [2–5]:

$$\mathbf{D}(\mathbf{r}) = \int \mathrm{d}\mathbf{r}'\epsilon(\mathbf{r},\mathbf{r}')\mathbf{E}(\mathbf{r}'). \tag{1}$$

In Fourier space, the dielectric function is therefore wavevector-dependent. In isotropic materials, the only relevant quantity is the longitudinal component $\mathbf{D}(\mathbf{q}) = \epsilon(\mathbf{q})\mathbf{E}(\mathbf{q})$, which can deviate substantially from the macroscopic, long wavelength limit ϵ. While stability requires that the macroscopic dielectric constant $\epsilon \geqslant 1$, the only forbidden range for $\epsilon(\mathbf{q})$ is $0 \leqslant \epsilon(\mathbf{q}) < 1$ [6].

The dispersion of $\epsilon(q)$ can be obtained from the correlation of polarization fluctuations $S(q)$ and the fluctuation dissipation theorem, $\epsilon(q) = 1/(1 - S(q)/k_\mathrm{B}T)$. However, reliable results for $S(q)$ from scattering experiments or computer simulations are difficult to obtain, and only a few results have recently become available. In the absence of tight experimental constraints, a popular starting point has therefore been to assume that polarization correlations decay exponentially over a length scale $1/q_0$, which lead to a Lorentzian form of the dielectric function [4]:

$$\epsilon(q) - 1 = 1/(\kappa + (q/q_0)^2). \tag{2}$$

This model has been extensively studied and already improves local electrostatics, since it interpolates between the

macroscopic continuum limit $\epsilon(q = 0) \equiv \epsilon = 1 + 1/\kappa$ and the correct limit $\epsilon(q \to \infty) = 1$. If the solvent is water or, more generally, a polar fluid, however, model calculations [7], neutron diffraction experiments and atomistic molecular dynamics simulations [8–10] have shown that the form of $\epsilon(q)$ is more complicated. Before decaying to 1 at large wavevectors, the dielectric function passes through two poles, and in between lies a band of negative values. The origin of this behavior is an overresponse or overscreening [11], so that the susceptibility $\chi(q) = 1 - 1/\epsilon(q) > 1$ for wavevectors q between 1 and 12 Å^{-1}.

The theory of nonlocal electrostatics is significantly more complicated to handle than the local approximation, since it involves a set of integro-differential equations; only the simplest geometries are analytically tractable. Molecular simulations with explicit solvent molecules take nonlocal correlations automatically into account, but all coarse-grained, implicit solvent models to date have completely ignored such effects due to the lack of computationally efficient techniques. An interesting proposition is the use of an auxiliary field that permits a reformulation in terms of partial differential equations in real space [12]. Using this approach, the Born solvation energy of ions was calculated with the approximation of equation (2). Although more complicated geometries can in principle be studied with this approach, it has not yet been widely applied.

Moreover, previous works on nonlocal electrostatics have only considered longitudinal correlations in the polarization field. Although these determine the longitudinal part of $\epsilon(\mathbf{q})$, transverse correlations are also present, as was recently confirmed by direct molecular dynamics simulations [13]. Since such correlations couple to the curl degrees of freedom of the polarization field $\mathbf{P}$, they can be expected to contribute in geometries where the field lines strongly deviate from spherical symmetry. No calculation has explored the importance of these effects so far.

In this paper, we study numerically nonlocal dielectric effects via a recently introduced nonlocal polarization energy functional that is capable of generating wavevector-dependent dielectric functions of both the form of equation (2) and additionally the main features of $\epsilon(\mathbf{q})$ in water [14], including overscreening. The model has been proposed to include nanoscale dielectric effects in implicit solvent simulations within a local Monte Carlo algorithm for charged systems [15]. A major attraction of this technique is that it is fairly easy to implement even in very complicated geometries and scales linearly with the number of charges in the system. Additionally, transverse polarization correlations can easily be included. We first apply this functional to a few generic situations in order to show that the approach agrees with earlier, well-known results for the importance of nonlocal electrostatics on the nanoscale: both pair potentials and solvation energies strongly deviate from their local values on scales of the order of a few ångströms. We then study situations that can no longer be treated analytically, in particular the important situation of ion translocation through a narrow channel surrounded by a low dielectric material. We show that the transverse polarization correlations become important and substantially increase the dielectric barrier and hence the channel resistance.

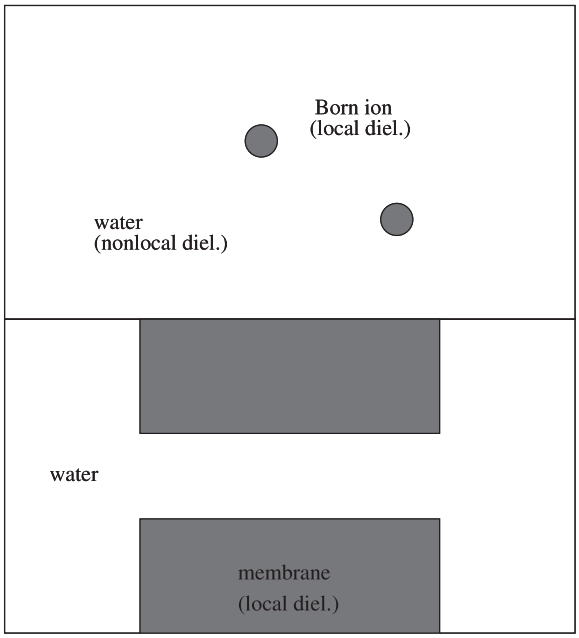

Figure 1. Typical geometries arising in electrostatic problems. Upper panel: Born ions of radius r correspond to a low dielectric sphere (gray) immersed in high dielectric water. Lower panel: a low dielectric membrane (gray) forms a molecular pore.

2. Model

We consider the electrostatic energy functional suggested in [14]:

$$U = \tfrac{1}{2}\int \mathrm{d}^3r[(\mathbf{D}-\mathbf{P})^2 + \kappa(r)\mathbf{P}^2 + \kappa_1(r)(\operatorname{div}\mathbf{P})^2 + \kappa_{\mathrm{tr}}(r)(\operatorname{curl}\mathbf{P})^2 + \alpha(r)(\operatorname{grad}\operatorname{div}\mathbf{P})^2] \quad (3)$$

supplemented by the Gauss constraint $\operatorname{div}\mathbf{D} = \rho$, where ρ is the charge density. Equation (2) can be viewed as a low order Landau–Ginzburg expansion of the electrostatic energy of polarization. If only the first two terms $(\mathbf{D}-\mathbf{P})^2$ and $\kappa(r)\mathbf{P}^2$ are present, conventional local electrostatics of continuous media with $\epsilon(\mathbf{r}) = 1 + 1/\kappa(\mathbf{r})$ is obtained at the minimum of U. The gradient terms generate in addition scale-dependent, nonlocal interactions of the polarization field. In general, the dielectric function resulting from the above energy functional is

$$\epsilon(q) = 1 + 1/(\kappa(\mathbf{r}) + \kappa_1(\mathbf{r})q^2 + \alpha(\mathbf{r})q^4). \quad (4)$$

The curl term coupling to the transverse degrees of freedom does not affect the longitudinal component of the dielectric function, but nevertheless contributes to the total electrostatic energy. The coefficients in front of the polarization terms describe the nature of the dielectric response of the material. For modeling a purely homogeneous solvent, no spatial dependence is needed. Figure 1 depicts typical situations, however, where different regions are occupied with different (mobile or immobile) dielectric matter, and modeling

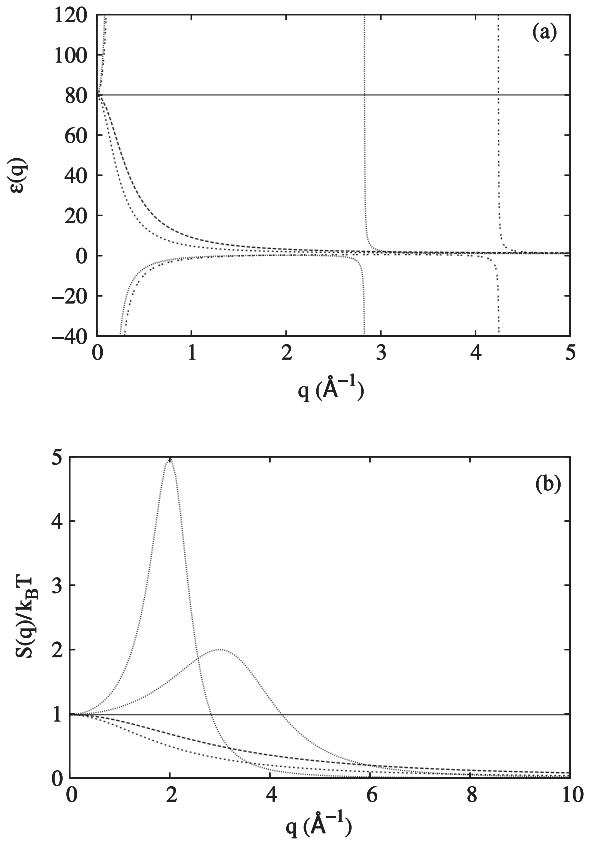

Figure 2. (a) Dielectric functions $\epsilon(q)$ used in this paper. Straight line local dielectric $\epsilon(q) \equiv \epsilon = 80$, other lines equation (4) for the Lorentzian model with $q_0 = 3$ Å^{-1} (thick dashed) and $q_0 = 2$ Å^{-1} (thin dashed), and the water model with $q_0 = 3$ Å^{-1}, $A = 2$ (double-dashed) and $q_0 = 2$ Å^{-1}, $A = 5$ (dotted). (b) Corresponding structure factors $S(q)/k_BT$ for the same sets of parameters. For the water model the height of the peak at q_0 is A.

the corresponding heterogeneous response requires different coefficients in different regions.

When setting $\kappa_1 = 1/q_0^2$ and $\alpha = 0$, we obtain equation (2), which will be referred to as the 'Lorentzian model' in the following. We assume equal strength of longitudinal and transverse correlations and set $\kappa_{tr} = \kappa_l$ throughout the paper. In the Lorentzian model, both κ_l and κ_{tr} must be positive for stability. When the expansion is truncated after the second-order grad div term, however, κ_l may be negative as long as the coefficient of the highest-order term α remains positive. It is now possible to select a characteristic wavelength q_0 for the spatial modulation of the polarization field, corresponding to a band of negative dielectric function (the overscreening effect), as can be seen in figure 2; we will refer to this model as the 'water model', equation (4).

An alternative to generating the overscreening effect in a Ginzburg–Landau Hamiltonian was suggested in [11]. In this work, the Hamiltonian is truncated at first order after the $(\mathrm{div}\,\mathbf{P})^2$ term, but contains two polarization fields, one of which is coupled to the gradient of a scalar order parameter field that may correspond to a local density. This formulation lends itself to a physical interpretation, in which overscreening arises from correlations between polarization and density. The present work shows that such a coupling is not necessary and the overscreening resonance can also be obtained from a single vectorial order parameter field if higher-order terms are included instead. Both the present approach and that of [11] describe linear response only; for an extension to nonlinear effects see [16, 17].

Figure 2(a) shows the five different dispersion relations studied in this work: a purely local dielectric with no dispersion, and two parameterizations for the Lorentzian and water models, respectively. In order to map the water model onto real solvents, it is convenient to parameterize the coefficients in terms of the position q_0 of the maximum of the (experimentally measurable) response function with amplitude A: the maximum of $S(q)/k_BT = 1-1/\epsilon(q)$ is located at $q_0^2 = -\kappa_1/2\alpha$ which fixes α in terms of κ_1, and setting $S(q_0)/k_BT = A$ determines $\kappa_1 = 2(1/A - \kappa - 1)/q_0^2$ in terms of q_0 and A. Figure 2(b) illustrates the response functions corresponding to the five dielectric functions. In this representation, the origin of the overscreening effect as a peak in the structure factor of the bound charge density is particularly visible.

For water with a macroscopic dielectric constant $\epsilon = 80$, the simulations of Bopp *et al* [8] suggest $q_0 = 3$ Å^{-1} and $A = 2$. However, subsequent work found that these values can be very sensitive to the local charge distribution of the water molecule and suggests instead $q_0 = 2$ Å^{-1}, $A = 5$ [18]. Given the variability of these results, a unique parameterization of equation (3) for water cannot be given at present. We therefore study both sets of parameters to explore the implications of this variability for physically measurable quantities. Both parameterizations are compatible with the forbidden region $0 \leqslant \epsilon(\mathbf{q}) < 1$. The electrostatic energy is discretized and minimized using Monte Carlo techniques; for details see the appendix.

3. Results

3.1. Ions in homogeneous solvent

We begin our demonstration of nonlocal dielectric effects in the simplest possible situation, a pair of ions of opposite charge in a uniform solvent described by equation (3). For a local dielectric, the energy for a pair of ions with charges $\pm e$ separated by a distance r is given by Coulomb's law:

$$U(r) = \frac{-e^2}{4\pi\epsilon_0\epsilon r} + \mathcal{O}\left(\frac{e^2r^2}{3\epsilon L^3}\right). \tag{5}$$

The quadratic correction has its origin in the periodic boundary conditions associated with the constrained electrostatic functional [19]. In figure 3, we show the electrostatic energy as a function of distance in five different dielectric backgrounds. The local dielectric agrees with equation (5). The Lorentzian model simply increases the attractive interaction at short distances, and more so for smaller wavevectors q_0. This trend can be expected from the fact that $\epsilon(q) < \epsilon$ for all nonzero wavevectors q; hence the ions see a smaller effective permittivity [4] and the energy increases. The behavior for the water model with its band of negative permittivity is much more spectacular and implies qualitatively different behavior.

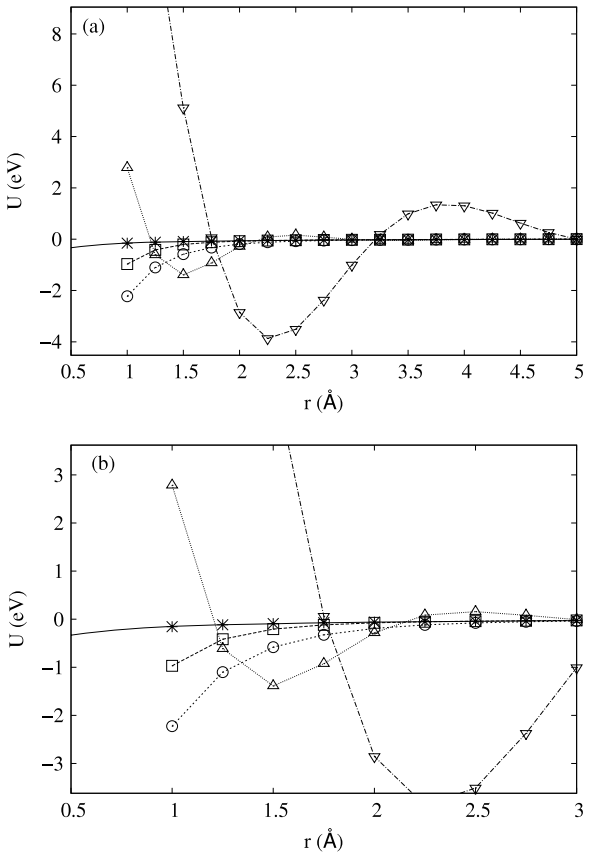

Figure 3. (a) Pair potential for oppositely charged ions. ⋆: local dielectric, □: Lorentzian model $q_0 = 3$ Å^{-1}, ○: Lorentzian model $q_0 = 2$ Å^{-1}, △: water model $q_0 = 3$ Å^{-1}, $A = 2$, ▽: water model $q_0 = 2$ Å^{-1}, $A = 5$. Solid line: expected behavior equation (5) for local electrostatics. (b) Close-up of the small-distance region.

We observe that the sign of the interaction is reversed at short distances and the potential exhibits damped oscillations that reach past 5 Å. Ions experiencing this potential in thermal equilibrium would be expected to populate the minima and the density should show oscillatory behavior. Although the presence of such potential oscillations in polar solvents has been pointed out many years ago [20, 4, 7], Coulomb's law (equation (5)) is still considered appropriate for interactions between point charges in implicit solvents.

3.2. Born ions in homogeneous solvent

In molecular simulations, ions are often not just modeled as point charges, but instead are represented as a point charge inside a spherical cavity of radius r from which the solvent is excluded. Inside the cavity, the dielectric permittivity is therefore that of free space, $\epsilon(q) = 1$, and the coefficients of the nonlocal terms vanish ($\kappa_l = \kappa_{tr} = \alpha = 0$). This model is known as the Born model of ions. Figure 4 explores the role of nonlocal dielectric response on the interaction between two such Born ions. We observe the same qualitative behavior already discussed for point charges. The Lorentzian model only increases the interaction at small scales, but the water model shows again strong oscillatory behavior and sign reversal at short distances.

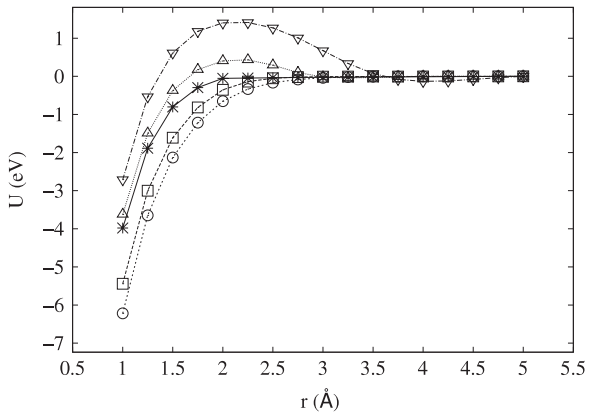

Figure 4. Pair potential for oppositely charged Born ions of radius $r = 1a$. ⋆: local dielectric, □: Lorentzian model $q_0 = 3$ Å^{-1}, ○: Lorentzian model $q_0 = 2$ Å^{-1}, △: water model $q_0 = 3$ Å^{-1}, $A = 2$, ▽: water model $q_0 = 2$ Å^{-1}, $A = 5$.

3.3. Born solvation energy

The Born solvation energy is the energy released when solvating a single Born ion inside a low dielectric sphere of radius r in high dielectric water. This quantity is of fundamental importance for the thermodynamics of electrolytes. If the solvating liquid is a local dielectric with permittivity ϵ, this energy has the well-known Born form [21]

$$U_{\text{Born}} = \frac{e^2}{8\pi\epsilon_0 r}\left(\frac{1}{\epsilon} - 1\right), \tag{6}$$

which is equivalent to the electrostatic energy of an ion in its own reaction field. The effect of nonlocal electrostatics on the Born solvation energy has already been investigated in previous work [22, 12]. Generally, U_{Born} is found to decrease relative to the value in a local dielectric for the Lorentzian model, but increases for the water model. Indeed, results from our present approach using the polarization energy functional are consistent with these trends. We place a single charge at the center of a low dielectric described by local electrostatics with $\epsilon = 1$ and vary the radius r of the dielectric sphere. Figure 5 plots this energy as a function of ion radius r. Note that, since our method requires charge neutrality, all energies are measured against a uniformly charged background of opposite sign. For the local dielectric, we recover approximately the $1/r$ behavior predicted by equation (6); the nonlocal terms lead to deviations. For an ion of radius $r = 1$ Å, figure 5 shows a decrease of the Born solvation energy by ∼30% for the Lorentzian model in qualitative agreement with, for example, [12]; the water model slightly increases the energy instead.

Experimentally measured Born solvation free energies are always lower than those predicted by equation (6) and hence in better agreement with the Lorentzian model than with the water model. It has been shown, however, that the overscreening resonance can be reconciled with experimental values by going to a smeared Born sphere, which should be a more realistic representation of ions in solution [22]. Additionally, the present results were obtained with linear response theory, and including nonlinear effects also leads to better agreement [17].

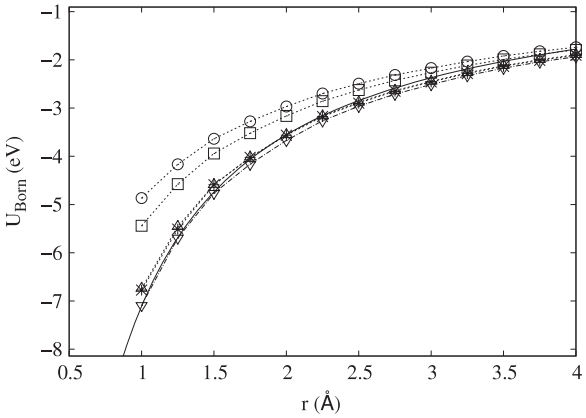

Figure 5. Born solvation energy for single charge in a dielectric sphere of radius r with smeared-out background for charge neutrality. ⋆: local dielectric, □: Lorentzian model $q_0 = 3$ Å^{-1}, ○: Lorentzian model $q_0 = 2$ Å^{-1}, △: water model $q_0 = 3$ Å^{-1}, $A = 2$, ▽: water model $q_0 = 2$ Å^{-1}, $A = 5$. Solid line: equation (6). Curves have been shifted by a constant offset so that (⋆) agree with equation (6) at large r.

3.4. Dielectric barrier for an ion channel

The electrostatic problems discussed so far were examples of highly symmetric, spherical geometries and could have also been studied analytically. Situations of experimental interest usually do not exhibit such symmetry, but can be addressed with equation (3) with no additional difficulty. A situation of great biological and technological importance is the transport of ions through a water-filled narrow channel formed by a low dielectric material. Ion channels in lipid membranes are truly nanoscopic devices with typical radii of 3–8 Å and a length of ∼50 Å, while artificial nanopores, for instance in silicon oxide films, are somewhat larger with radii $r_{ch} \sim 10$ Å and tens of nanometers in length [23]. In both cases, the dielectric permittivity of the channel-forming material is between $\epsilon_m = 2$–4, which creates a huge contrast to the surrounding water at $\epsilon_w = 80$.

Due to the dielectric contrast, the energy of an ion inside a channel is much higher than in a homogeneous solvent environment. The field lines are mostly confined to the high dielectric region, and the electrostatic energy rises linearly with charge separation. The energy difference between an ion inside and outside the channel is referred to as the dielectric barrier and fundamentally controls the conductivity of the channel [24]. It has been the subject of much current research and has been calculated on the level of fully atomistic molecular dynamics [25] and highly idealized geometries using continuum electrostatics [26, 27].

The simplest model of an ion channel consists of a cylindrical region of water of radius r_{ch} embedded in a low dielectric medium. For an infinite channel described by two local dielectrics ϵ_w inside the channel and ϵ_m outside the channel, the electrostatic calculations of [28] estimate the dielectric barrier

$$U_\infty \approx \frac{e^2\sqrt{2(\log(2\xi/r_{ch}) - 0.577)}}{8\pi\epsilon_0\sqrt{\epsilon_w\epsilon_m}r_{ch}} - \frac{0.13e^2}{8\pi\epsilon_0\epsilon_m\xi}, \qquad (7)$$

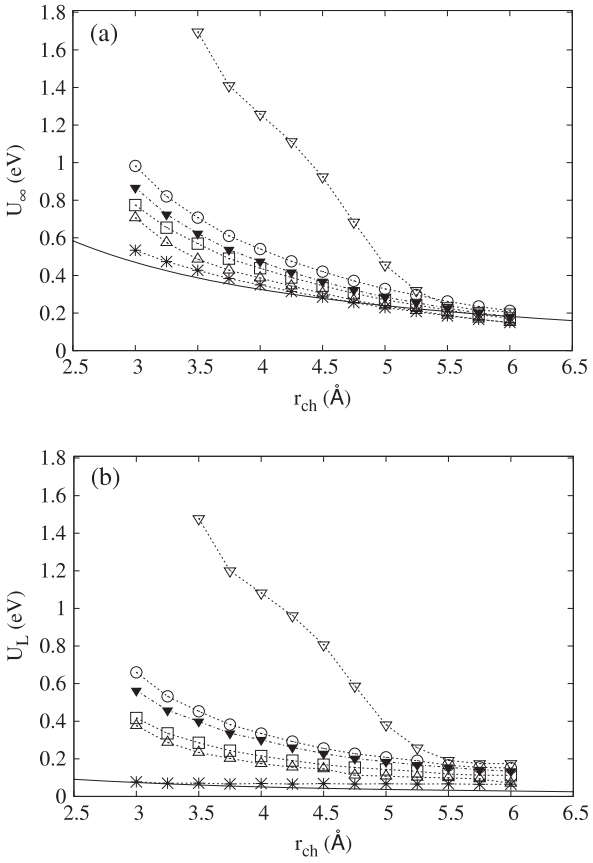

Figure 6. Dielectric barrier for a cylindrical ion channel of radius r_{ch} and $\epsilon_m = 1$ with smeared-out background for charge neutrality. (a) Infinite channel, (b) finite channel of length $L = 3r$. ⋆: local dielectric, □: Lorentzian model $q_0 = 3$ Å^{-1}, ○: Lorentzian model $q_0 = 2$ Å^{-1}, △: water model $q_0 = 3$ Å^{-1}, $A = 2$, ▽: water model $q_0 = 2$ Å^{-1}, $A = 5$. Also shown are results for the local dielectric and transverse correlations ($q_0 = 2$ Å^{-1}) (▼). Solid line: equations (7) and (8).

where ξ must be determined from the transcendental equation $\xi^2 = r_{ch}^2(\epsilon_w/2\epsilon_m)(\ln(2\xi/r_{ch}) - 0.577)$. Similarly, for a finite channel of length L the barrier is approximately

$$U_L \approx U_\infty(1 - \exp(-L/2\xi)). \qquad (8)$$

According to these expressions, the barrier for an infinite channel varies $\sim 1/r_{ch}$; the same holds true for a finite channel if $L \propto r_{ch}$.

The only available study of nonlinear effects on the translocation barrier has been limited to the Lorentzian model in the analytically solvable situation of an infinite slab or cylinder [29, 30]. In figure 6 we calculate the dielectric barrier as the energy difference between a single ion centered in the middle of a channel and the same ion solvated by pure water for channel radii varying from 3 to 6 Å. Panel (a) shows results for an infinite channel, which is often taken as an approximation for a very long channel, while panel (b) examines the opposite limit of a very short channel. This geometry is no longer analytically solvable. Inside the channels, the dielectric is described by the full equation (3), while outside the channel

we set $\kappa_l = \kappa_{tr} = \alpha = 0$. This implies that the dielectric profile changes from that of a local electrostatic in the membrane to that of water over the scale of one mesh spacing h. For the local dielectric, numerical results agree quite well with the approximations of equations (7) and (8); exact agreement should not be expected due to the boundary conditions and the uniform countercharge. Interestingly, all nonlocal approximations increase the dielectric barrier over the local value to varying extent. A significant part of this increase is due to the $(\mathrm{curl}\,\mathbf{P})^2$ term in equation (3), which is evidenced by the (▼) data that is based on the local approximation and the $(\mathrm{curl}\,\mathbf{P})^2$ term only. In our model, the dielectric barrier typically doubles or triples for small radii. A much larger effect is seen for the water model with $q_0 = 2$ Å^{-1}, $A = 5$, where the barrier rises strongly above the local value. This result underlines the strong sensitivity of the results to the parameterization of the energy functional. Once the channel radii reach ∼6 Å the barriers begin to reach the local value and nonlocal effects cease to be important. We note that one cannot expect equation (3) to describe ultrasmall channels that would only fit single water molecules.

4. Discussion

We have computed nonlocal electrostatic effects on the level of a linear polarization free energy functional that yields a dielectric permittivity with the main features of water in several standard geometries. Additionally, it includes transverse correlations of the polarization field that were not present in earlier treatments of nonlocal dielectric response. In isotropic systems, our approach reproduces, in agreement with earlier work [4], that the Coulomb interaction on distances <5 Å is strongly altered by a permittivity that includes a band of negative values at finite wavevectors. The potential between bare ions is no longer purely attractive, but exhibits damped oscillations at short distances and can therefore change sign. These oscillations may be unimportant in dilute salt solutions where the ions are far away from each other, but should alter the structure of a condensed counterion cloud around strongly charged colloids or polyelectrolytes [31].

Also in agreement with previous results from nonlocal electrostatic theory, the Born solvation energy U_{Born} increases relative to the local electrostatic result. Since the local dielectric approximation already overestimates experimental Born solvation energies, linear nonlocal response cannot be invoked to explain this discrepancy. This finding, however, does not imply that nonlocal electrostatics is at odds with experiments. Relatively simple improvements such as considering a smeared Born sphere or nonlinear effects already lead to much better agreement. More recently, it has been pointed out that the modified solvent structure in the vicinity of a solvated ion can also play a role [32]. Using integral equation theory, very good agreement with U_{Born} for monovalent ions was achieved.

Finally, models of ion channels based on purely local electrostatics would underestimate the dielectric barrier. Moreover, nonlocal models not including transverse correlations would miss a large fraction of this effect. Since the resistivity of an ion channel depends exponentially on the magnitude of the dielectric barrier, it may be quite sensitive to nonlocal interactions. As in the case of solvation, however, experimental barriers are much lower than even those obtained from local electrostatics, so that other effects, such as screening by salt or decoration of channel walls with charges [33], must be invoked to explain why membrane channels exhibit the measured ion conductivities.

Nonlocal electrostatics is usually completely ignored in implicit solvent simulations of charged soft matter systems. The local polarization functional provides a relatively simple way to include such effects in Monte Carlo simulations and could in principle be generalized to molecular dynamics. A limitation is the current uncertainty in the parameterization of the functional. Atomistic simulations measuring the dielectric function are involved and the results are sensitive to the type of water model used in the computations. In light of the results of [32], it seems necessary to take into account local distortion of the solvent in the vicinity of charges, which could readily be done using the spatially varying coefficients in the energy functional. Additionally, the dielectric behavior of interfacial water is likely different from that of bulk water and may have to be described by a smooth interpolation from bulk water to bulk membrane dielectric. Further molecular dynamics studies similar to those for bulk water [8], but in the presence of low dielectric boundaries, are needed to reliably parameterize the functional near interfaces so that fully quantitative modeling can be performed.

Acknowledgments

This work benefited greatly from many stimulating discussions and helpful advice from A C Maggs, who also pointed out the relevance of transverse polarization correlations for ion channel geometries. We also thank the Natural Sciences and Engineering Research Council of Canada (NSERC) for financial support.

Appendix. Numerical discretization of the energy functional

For numerical simulation, we discretize the energy equation (3) on a periodic cubic mesh of size L with mesh spacing $a = 0.25$ Å. As illustrated in figure A.1, it is natural to interpolate the vectorial fields $\mathbf{D}$ and $\mathbf{P}$ onto the links that emanate from the vertices $n = (i, j, k)$, and we denote the components in a Cartesian direction δ on vertex n with D^n_δ and P^n_δ, resp. The (scalar) divergence of $\mathbf{P}$ is then associated with the vertices, $(\mathrm{div}\,\mathbf{P})^n$ and the gradient of the divergence again with the links connecting two vertices, $(\mathrm{grad}\,\mathrm{div}\,\mathbf{P})^n_\delta$. The components of the curl of $\mathbf{P}$, however, are associated with the normal of the face formed by four links each and denoted by $(\mathrm{curl}\,\mathbf{P})^n_\delta$. The discretized energy then is

$$U = \frac{a^3}{2} \sum_{n=(i,j,k)} \sum_{\delta=x,y,z} [(D^n_\delta - P^n_\delta)^2 + \kappa^n_\delta (P^n_\delta)^2 + \kappa^n_l [(\mathrm{div}\,\mathbf{P})^n]^2 + \kappa^n_{\mathrm{tr},\delta} [(\mathrm{curl}\,\mathbf{P})^n_\delta]^2 + \alpha^n_\delta [(\mathrm{grad}\,\mathrm{div}\,\mathbf{P})^n_\delta]^2], \quad (9)$$

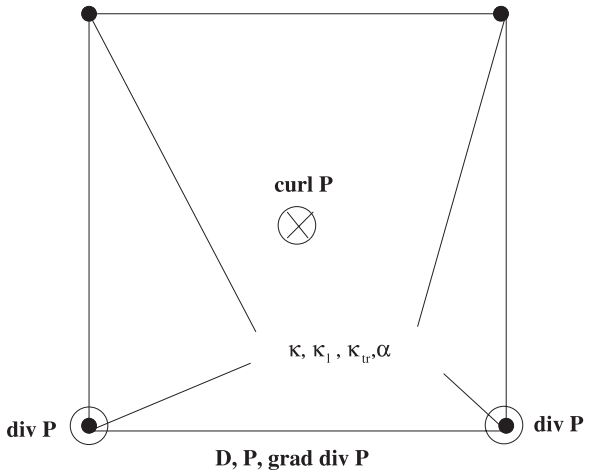

Figure A.1. Discretization of the energy functional equation (3) onto a cubic mesh. The vectorial quantities **D** and **P** are associated with the links connecting the vertices of the lattice. The scalar quantity div **P** is associated with the vertices and the vector curl **P** is associated with the faces of the mesh. The spatial fields $\kappa(r)$, $\kappa_{\rm l}(r)$, $\kappa_{\rm tr}(r)$ and $\alpha(r)$ are all discretized onto lattice vertices.

where the summation runs over all vertices and links (ijk) and three Cartesian directions δ. For the discretized curl, div and grad operators we use finite differences involving nearest-neighbor sites only.

The spatially varying coefficients $\kappa(\mathbf{r})$, $\kappa_{\rm l}(\mathbf{r})$, $\kappa_{\rm tr}(\mathbf{r})$ and $\alpha(\mathbf{r})$ are also discretized onto the vertices of the mesh. While the coefficient $\kappa_{\rm l}$ can be directly used in the scalar $(\mathrm{div}\,\mathbf{P})^2$ term in the discretized energy, an additional interpolation step is necessary to obtain discretized coefficients for the vectorial quantities associated with the links. The coefficients κ_δ^n and α_δ^n are therefore arithmetic averages over the values of the coefficients on the two nodes connecting the link in direction δ. For x-directed links, for instance, $\kappa_x^{(i,j,k)} = (\kappa^{(i,j,k)} + \kappa^{(i+1,j,k)})/2$ and $\alpha_x^{(i,j,k)} = (\alpha^{(i,j,k)} + \alpha^{(i+1,j,k)})/2$; analogous expressions hold for the y and z directions. Finally, the coefficient $\kappa_{{\rm tr},\delta}^n$ multiplying the curl is an arithmetic average over the values of $\kappa_{\rm tr}^n$ on the four vertices that form the plaquette with surface normal in the δ direction.

Having discretized the energy, the charge density $\rho(\mathbf{r})$ must also be interpolated onto the mesh. While full off-lattice schemes have been demonstrated in previous work [19, 34], we restrict ourselves here to a lattice gas and place the charge density directly onto the vertices, i.e. $\rho^n = q/a^3$. This does not pose a serious restriction, as we are interested in demonstrating nonlocal electrostatic effects in static situations only. In a constrained Monte Carlo simulation at finite temperature, both particles and all field degrees of freedom would undergo transitions with Metropolis rates. Here, we minimize the energy equation (9) with respect to **D** and **P** for a fixed charge configuration. In this minimization, we initialize the displacement field **D** so that it satisfies Gauss's law and then operate on its curl degrees of freedom only; the Gauss constraint hence remains satisfied. The polarization **P** is unconstrained and varied accordingly. Global minimization proceeds by repeated local minimization of the energy functional. For improved efficiency, a third type of Monte Carlo move is useful that consists in a combined update of curl **P** and curl **D**. This move separately minimizes the terms proportional to $\mathbf{P}^2$ and $(\mathrm{curl}\,\mathbf{P})^2$ only while leaving all other terms invariant.

References

[1] Landau L D and Lifshitz E M 1999 *Electrodynamics of Continuous Media* (Oxford: Pergamon)
[2] Dogonadze R R and Kornyshev A A 1974 *J. Chem. Soc. Faraday Trans.* II **70** 1121
[3] Kornyshev A A 1981 *Electrochim. Acta* **26** 1
[4] Kornyshev A A 1985 *The Chemical Physics of Solvation. Part A: Theory of Solvation* ed R R Dogonadze, R Kalman, A A Kornyshev and J Ulstrup (Amsterdam: Elsevier) p 77
[5] Mennucci B and Cammi R (ed) 2008 *Continuum Solvation Models in Chemical Physics: From Theory to Applications* (New York: Wiley)
[6] Dolgov O V, Kirzhnits D A and Maksimov E G 1983 *Rev. Mod. Phys.* **53** 81
[7] Raineri F O, Resat H and Friedman H L 1992 *J. Chem. Phys.* **96** 3068
[8] Bopp P A, Kornyshev A A and Sutmann G 1996 *Phys. Rev. Lett.* **76** 1280
[9] Bopp P A, Kornyshev A A and Sutmann G 1998 *J. Chem. Phys.* **109** 1939
[10] Olmelyan I P 1999 *Mol. Phys.* **96** 407
[11] Kornyshev A A, Leikin S and Sutmann G 1997 *Electrochim. Acta* **42** 849
[12] Hildebrandt A, Blossey R, Rjasanow S, Kohlbacher O and Lenhof H P 2004 *Phys. Rev. Lett.* **93** 108104
[13] Olmelyan I P 1998 *Mol. Phys.* **93** 123
[14] Maggs A C and Everaers R 2006 *Phys. Rev. Lett.* **96** 230603
[15] Maggs A C and Rossetto V 2002 *Phys. Rev. Lett.* **88** 196402
[16] Kornyshev A A and Sutmann G 1997 *Phys. Rev. Lett.* **79** 3435
[17] Kornyshev A A and Sutmann G 1998 *J. Electroanal. Chem.* **450** 143
[18] Kornyshev A A and Sutmann G 1999 *J. Mol. Liq.* **82** 151
[19] Rottler J and Maggs A C 2004 *J. Chem. Phys.* **120** 3119
[20] Holub K and Kornyshev A A 1980 *J. Chem. Soc. Faraday Trans.* II **76** 67
[21] Born M 1920 *Z. Phys.* **1** 45
[22] Kornyshev A A and Sutmann G 1996 *J. Chem. Phys.* **104** 1524
[23] Kamenev A, Zhang J, Larkin A I and Shklovskii B I 2006 *Physica* A **359** 129
[24] Parsegian A 1969 *Nature* **221** 844
[25] Roux B, Allen T, Berneche S and Im W 2004 *Q. Rev. Biophys.* **37** 1
[26] Levitt D G 1978 *Biophys. J.* **22** 209
[27] Jordan P C 1982 *Biophys. J.* **39** 157
[28] Teber S 2005 *J. Stat. Mech.* P07001
[29] Kornyshev A A, Tsitsuashvili G I and Yaroshchuk A E 1998 *Sov. Electrochem.* **25** 923
[30] Kornyshev A A, Tsitsuashvili G I and Yaroshchuk A E 1998 *Sov. Electrochem.* **25** 932
[31] Limbach H J, Holm C and Kremer K 2002 *Europhys. Lett.* **60** 566
[32] Fedorov M V and Kornyshev A A 2007 *Mol. Phys.* **105** 1
[33] Zhang J, Kamenev A and Shklovskii B I 2005 *Phys. Rev. Lett.* **95** 148101
[34] Maggs A C 2005 *Phys. Rev.* E **72** 040201